Lawrence Berkeley National Laboratory
LBL Publications

Title
Time-scale and Branching Ratios in Sequential Multifragmentation

Permalink
https://escholarship.org/uc/item/9043j1kp

Authors
Moretto, L.G.
Phair, L.
Tso, K.
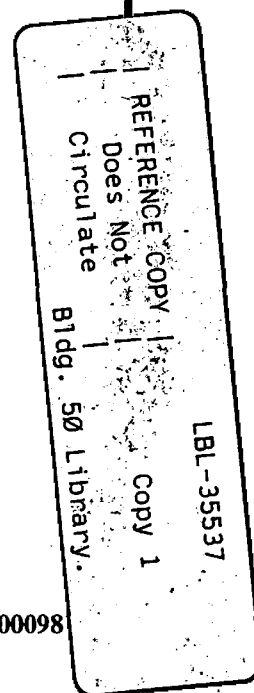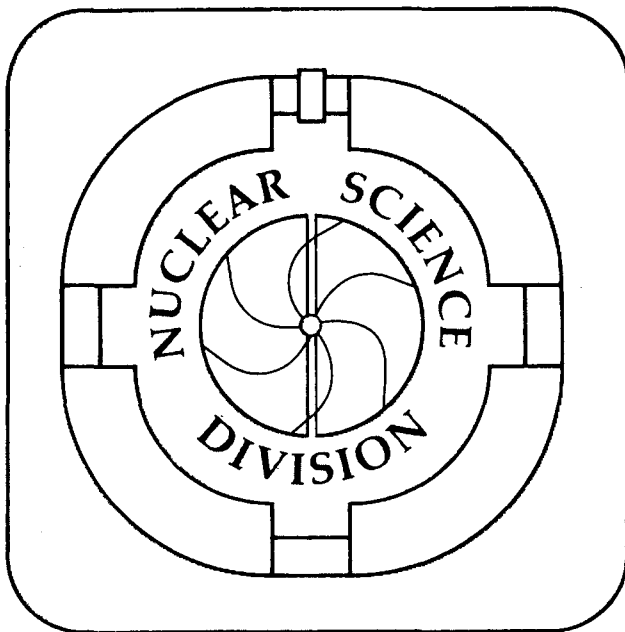et al.

Publication Date
1994-04-30

Lawrence Berkeley Laboratory
UNIVERSITY OF CALIFORNIA

Time-scale and Branching Ratios in
Sequential Multifragmentation

L.G. Moretto, L. Phair, K. Tso, K. Jing, and G.J. Wozniak

April 1994

DISCLAIMER

Time-scale and Branching Ratios in Sequential Multifragmentation

L.G. Moretto, L. Phair, K. Tso, K. Jing, and G.J. Wozniak

Nuclear Science Division
Lawrence Berkeley Laboratory
University of California
Berkeley, California 94720

April 1994

Time-scale and Branching Ratios in Sequential Multifragmentation

L. G. Moretto, L. Phair, K. Tso, K. Jing, and G. J. Wozniak

Nuclear Science Division, Lawrence Berkeley Laboratory, Berkeley, CA 94720

Abstract: Experimental intermediate-mass-fragment multiplicity distributions are shown to be binomial at all excitation energies. From these distributions a single binary event probability can be extracted that has the thermal dependence $p = \exp[-B/T]$. Thus, it is inferred that multifragmentation is a sequence of thermal binary events. The increase of p with excitation energy implies a corresponding contraction of the time-scale and explains recently observed fragment-fragment and fragment-spectator Coulomb correlations.

At low excitation energies, complex fragments are emitted with low probability by a compound nucleus mechanism[1-3]. At increasingly larger energies, the probability of complex fragment emission increases dramatically, until several fragments are observed within a single event [4-9]. The nature of this multifragmentation process is at the center of much current attention. In particular, the issue of sequentiality versus simultaneity is hotly debated theoretically[4-12], and is the object of intense experimental study[13-21].

This polarization is evident even within the framework of statistical theories. On the one hand, sequential multifragmentation theories allow the fragments present at any stage to undergo additional binary decays with probabilities determined from more or less standard compound nucleus decay widths[22, 23]. On the other hand, chemical equilibrium-like theories generate fragments in chemical equilibrium, and release them simultaneously when the average density of the system falls below a critical freeze out value[5, 8, 10, 24, 25].

Recent experimental work [26, 27] has shown that the excitation functions for the production of two, three, four, etc. fragments have a characteristically statistical energy dependence. However the issue of sequentiality versus simultaneity could not be resolved. Several efforts to settle this dispute have utilized the pairwise fragment-fragment correlations introduced by their mutual Coulomb interaction. Results have been presented showing a substantial dip in the probability of finding pairs of fragments at small relative velocities[15-19] and small relative angles[13, 14, 20]. Simulations, performed with chemical equilibrium and sequential decay codes, were compared with experiment, and the rather short upper limits obtained for the decay time-scales were deemed consistent with a simultaneous break up.

A recent experiment[20] has studied the "proximity" effect of the surviving partner, produced in a deep inelastic-like collision, on the angular distribution of the fragments resulting from the break-up of the other partner. In this experiment the measured total kinetic energy loss of the primary binary collision can be related to the excitation energy of the nucleus undergoing multifragmentation. This remarkable experiment shows that at small excitation energies the "proximity" effects are essentially absent, but become very pronounced at large excitation

energies. This onset of proximity effects was taken to signify a transition from "conventional" sequential multifragmentation to "true" simultaneous multifragmentation.

The conclusions drawn from these experiments are predicated upon the tacit assumption that sequential decay always occurs on a very long time scale, so that the large space-time separation of sequentially emitted fragments makes their interaction negligible. This (incorrect) assumption has been consistently incorporated into simulations based upon sequential emission codes.

In what follows we shall show three things.

First, the usual thermal binary probabilities associated with sequential emission undergo a dramatic increase with excitation energy and the corresponding emission time-scale contracts dramatically, in agreement with observation[16, 17, 19, 20]. This is a very relevant, though straightforward and in many ways somewhat trivial point.

Second, the sequential time-scale and its contraction with excitation energy are directly related to the excitation functions for binary, ternary, quaternary, etc., decays through the elementary binary decay probability.

Third, we can extract this elementary binary decay probability and the corresponding time scale from the experimental excitation functions.

The first point is readily shown. For statistical decay one can rewrite the partial decay width Γ in terms of a partial decay time τ. The partial decay width associated with a given channel can be written as:

$$\Gamma = \hbar \omega_o e^{-B/T},\tag{1}$$

where ω_o is a frequency characteristic of the channel under consideration, B is the barrier associated with the channel, and T is the temperature. For instance, in fission ω_o is the collective frequency of assault on the barrier ($\sim$ beta vibration frequency) and B is the fission barrier.

The elementary probability p for a binary decay to occur at any given "try" defined by the channel period $\tau_o = 1 / \omega_o$ is:

$$p = \frac{\Gamma}{\hbar \omega_o} = e^{-B/T}.\tag{2}$$

The corresponding time is given by:

$$\tau = \tau_o e^{B/T}.\tag{3}$$

In the case of a compound nucleus, the total decay width is the sum of the widths of all channels, and the lifetime is calculated accordingly. This lifetime defines the survival of the initial unmodified compound nucleus. For sequential multifragmentation, only the decay width and lifetime for binary fragment formation need be considered, while the abundant light particle decay can be treated as a background that progressively decreases the temperature and possibly the barrier.

2

Equation 3 shows that the decay lifetime is dramatically affected even by moderate changes in temperature. For a binary fission-like decay with a barrier of approximately 20 MeV, a change in temperature from 2 to 5 MeV decreases the lifetime by a factor of 400 and increases the binary decay probability accordingly! Furthermore, as the temperature becomes comparable with the barrier, the binary decay probability approaches unity and the lifetime approaches the characteristic (dynamical) time constant of the channel, τ_o.

We argue that this dramatic decrease of the decay lifetime with increasing excitation energy is the effect observed in Refs. [16, 17, 19, 20], and that *this effect is inherent to the energy dependence of sequential decay, rather than a transition from sequential to true multifragmentation*. If this is indeed the case, there is no need for a separate theory of multifragmentation, since this process is reducible to a sequence of binary decays that can be described in a standard way.

As a second point, we note that the elementary binary probability p (or the time τ) can be directly related to the experimental branching ratios for binary, ternary, quaternary, etc., decay. For simplicity, let us assume that the system has the opportunity to try m times to emit an "inert" fragment with constant probability p. The probability P_n^m of emitting exactly n fragments is given by the binomial distribution:

$$P_n^m = \frac{m!}{n!(m-n)!} p^n (1-p)^{m-n}.$$ (4)

The average multiplicity is then

$$\langle n \rangle = mp$$ (5)

and the variance

$$\sigma_n^2 = \langle n \rangle (1-p).$$ (6)

Thus, from the experimental values of $\langle n \rangle$ and σ_n^2 one can extract values for p and m, at any excitation energy. Alternatively, one can extract p from the ratio of any pair of excitation functions $P_n^m(T)$:

$$\frac{1}{p} = \frac{\tau}{\tau_o} = \frac{P_n^m}{P_{n+1}^m} \frac{m-n}{n+1} + 1.$$ (7)

We now proceed to verify the above predictions by comparison with experiment. References [28, 29] report values of $\langle n \rangle$ and σ_n^2 for the reaction ^{36}Ar + ^{197}Au at 80 & 110 MeV/u (available center-of-mass energy of 2.4 and 3.3 GeV, respectively) as a function of the transversal energy E_t of the event,

$$E_t = \sum \varepsilon_i \sin^2 \theta_i,$$ (8)

3

where ε_i is the kinetic energy of each fragment and θ_i is the angle between the fragment and the beam direction. In choosing the transversal energy as our observable, we assume that it is proportional to the excitation energy of the source E[30]

$$E_t = K(E, A_P, A_T)E$$ (9)

From Equations 5 and 6, we extract the elementary probability p and m from the mean and variance of the experimental multiplicity distributions[28, 29] for the ^{36}Ar + ^{197}Au reactions at E/A=80 and 110 MeV. At this point we need to consider the effect of the device efficiency ε on the fold probabilities, the mean multiplicity and its variance, and finally, on the observed probability p_{obs}. Disregarding details associated with anisotropies, multiple hits, etc, we can estimate that the true probability p is simply related to the observed probability p_{obs} by the relationship:

$$p_{obs} = \varepsilon p$$ (10)

This observed probability p_{obs} should combine exactly like p in the binomial expressions (Equations. 4 - 7). The geometric efficiency of the Miniball is 0.89 [31] and represents an upper limit for the device efficiency in the experiment quoted above. The derived values of p_{obs} should be corrected by the device efficiency ε to obtain the physical probability p.

In Figure 1 we plot m as a function of E_t for the intermediate mass fragment ($3 \leq Z \leq 20$) multiplicity distributions (circles) and the total charged particle multiplicity distributions (diamonds). In Figure 2, we plot $ln\ 1/p$ vs. $E_t^{-\frac{1}{2}}$ for the fragment distributions. If the probability p is statistical, as given in Equations (2), this plot ought to be linear[26] since $T \propto \sqrt{E}$. The linearity of this plot over two orders of magnitude is stunning, and leaves little doubt regarding the "thermal" nature of p.

The dramatic contraction of the time scale down to values close to the characteristic channel time shows that the onset of fragment-fragment or spectator-fragment interactions at high excitation energy is a natural consequence of Equations (2) and (3). The difference in slope for the two bombarding energies strongly suggests that the simple proportionality law of Equation (9) is well satisfied.

One could also extract p "differentially" (Equation (7)) by considering the ratios P_n / P_{n+1} from the unpublished experimental excitation functions[32]. Although we have not been granted permission to use these unpublished data, we can state that up to $n = 8$ all of the experimental excitation functions tightly collapse onto the two straight lines shown in Figure 2, when subjected to the above procedure. We can however show the calculated excitation functions (see Figure 3) using the values of m and p from Figures 1 and 2 and vouch for the extraordinary quantitative agreement between the calculations and the experimental data.

Preliminary analysis of two additional experiments [33, 34] with different target-projectile combinations and bombarding energies confirms the general applicability of this description. The *rigorous* applicability of the binomial distribution is very powerful evidence for the reducibility of the n-fold probabilities P_n to the elementary binary probability p and for the sequential structure of the multifragmentation event. The linearity of the extracted elementary binary probability plot (see Fig. 2) over two orders of magnitude is truly stunning, and indicates the

4

thermal nature of the process at all excitation energies. The associated time-scale demonstrates the expected smooth contraction in time with increasing excitation energy without any indication of a new mechanism appearing at the highest energies.

The more directly interpretable physical parameter contained in this analysis is the binary barrier B (proportional to the slope of the data in Figure 2). One may wonder why a single binary barrier suffices, since mass asymmetries with many different barriers may be present. This is an old problem. Let us consider a barrier distribution as a function of mass asymmetry x of the form:

$$B = B_o + ax^n,$$

(11)

where B_o is the lowest barrier in the range considered. Then,

$$p = \frac{\Gamma}{\hbar\omega_o} = \int e^{-B_o/T} e^{-ax^n/T} dx \cong \left(\frac{T}{a}\right)^{1/n} e^{-B_o/T}.$$

(12)

Thus the simple form of Equations (1) and (2) is retained with a small pre-exponential modification.

The detailed accuracy and the broad applicability of the binomial distributions is somewhat disconcerting. For instance, what is the significance of the parameter m? In the present description the system is given m chances to emit a fragment, with fixed probability p, after which the emission is shut off. One might have guessed that the probability p would decrease progressively as a function of time due to evaporative cooling, and that m is just an approximate cut-off made necessary by the constant p in the binomial distribution. This hypothesis, however, may not be correct. A simple evaporation calculation shows that during the time $t = m\tau_0$ ($\hbar\omega_o \cong 1$ MeV) the system has little time to cool. Therefore p is truly constant and one is led to attribute a more physical significance to m. What switches the emission off after m tries must remain here a speculation. Let us venture to say that dynamics may be responsible for such an effect. Could it be that the fragments are statistically emitted while the system undergoes an expansion phase [35] only to be shut off as it reverts to normal density? If it were to be so, this would be the first significant dynamical feature in an otherwise utterly thermal picture.

In support of this view are the results of the same analysis on the total charged particles emitted in the same reactions. From the reported means and variances [29], one obtains values of m almost four times larger than those obtained for the fragments (see Figure 1). This suggests that the light charged particles are emitted over a much longer time which is in good agreement with the calculated cooling time.

We have tried to find alternative explanations for the binomial distributions with thermal probabilities. An obvious model is a chain of m links with probability p that any of the links is broken. The probability that n links are broken is given by Equation (4). This result is, of course, strictly dependent on the dimensionality of the model, and its relevance to multifragmentation is unclear. Nevertheless, it stresses again the *fundamental reducibility* of the multifragmentation probability to a binary breakup probability.

In summary:

1) The multifragment emission probability is rigorously binomial and is reducible to an elementary binary probability applied sequentially.

2) This binary elementary probability is "thermal", as demonstrated by its characteristic energy dependence.

3) The time scale of sequential emission contracts rapidly with increasing excitation energy as demanded by point 2). This contraction naturally explains the observed rapid onset of the fragment-fragment Coulomb interaction with increasing excitation energy and obviates the need for "simultaneous" multifragmentation as a distinct process.

4) The parameter m could be truly a physical quantity rather than an artificial cutoff. It may indicate a dynamical time interval during which fragments are thermally emitted with high probability (transient expansion phase?)

Acknowledgments

Figure Captions

Figure 1: The extracted values of $m = \langle n \rangle^2 / \left(\langle n \rangle - \sigma_n^2 \right)$ as a function of the transverse energy E_t for the reaction ^{36}Ar + ^{197}Au at E/A=80 MeV (open symbols) and 110 MeV (solid symbols). The circles correspond to m values extracted from the intermediate mass fragment distributions ($3 \leq Z \leq 20$)[28] while the diamonds correspond to m values extracted from the total charged particle distributions[29].

Figure 2: The reciprocal of the binary decay probability $1/p$ or the ratio τ / τ_o (calculated from the mean and variance of the intermediate mass fragment distributions) as a function of $E_t^{-\frac{1}{2}}$ for the reaction ^{36}Ar + ^{197}Au at E/A=80 MeV (open circles) and 110 MeV (solid circles). The solid lines are linear fits to $\log(1/p)$.

Figure 3: The calculated probability to emit n intermediate mass fragments ($3 \leq Z \leq 20$) as a function of E_t for the reaction ^{36}Ar + ^{197}Au at E/A=80 MeV (lower panel) and 110 MeV (upper panel). For numbers of fragments n=0-8, $P(n)$ is calculated assuming a binomial distribution (see Equation (4)) with the values of m and p shown in Figures 1 and 2.
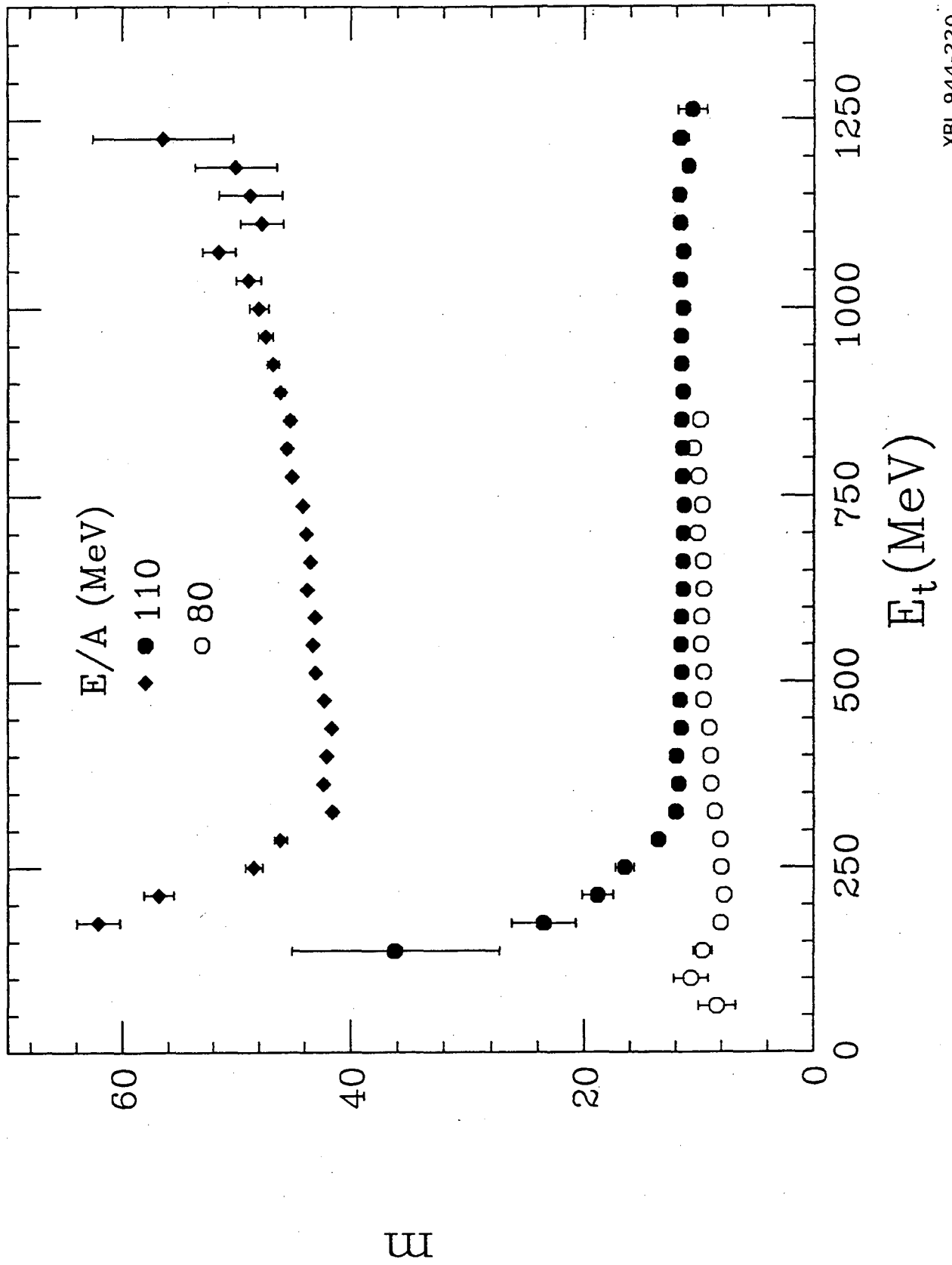
References

[1] L. G. Sobotka et al., Phys. Rev. Lett. 51, 2187 (1983).

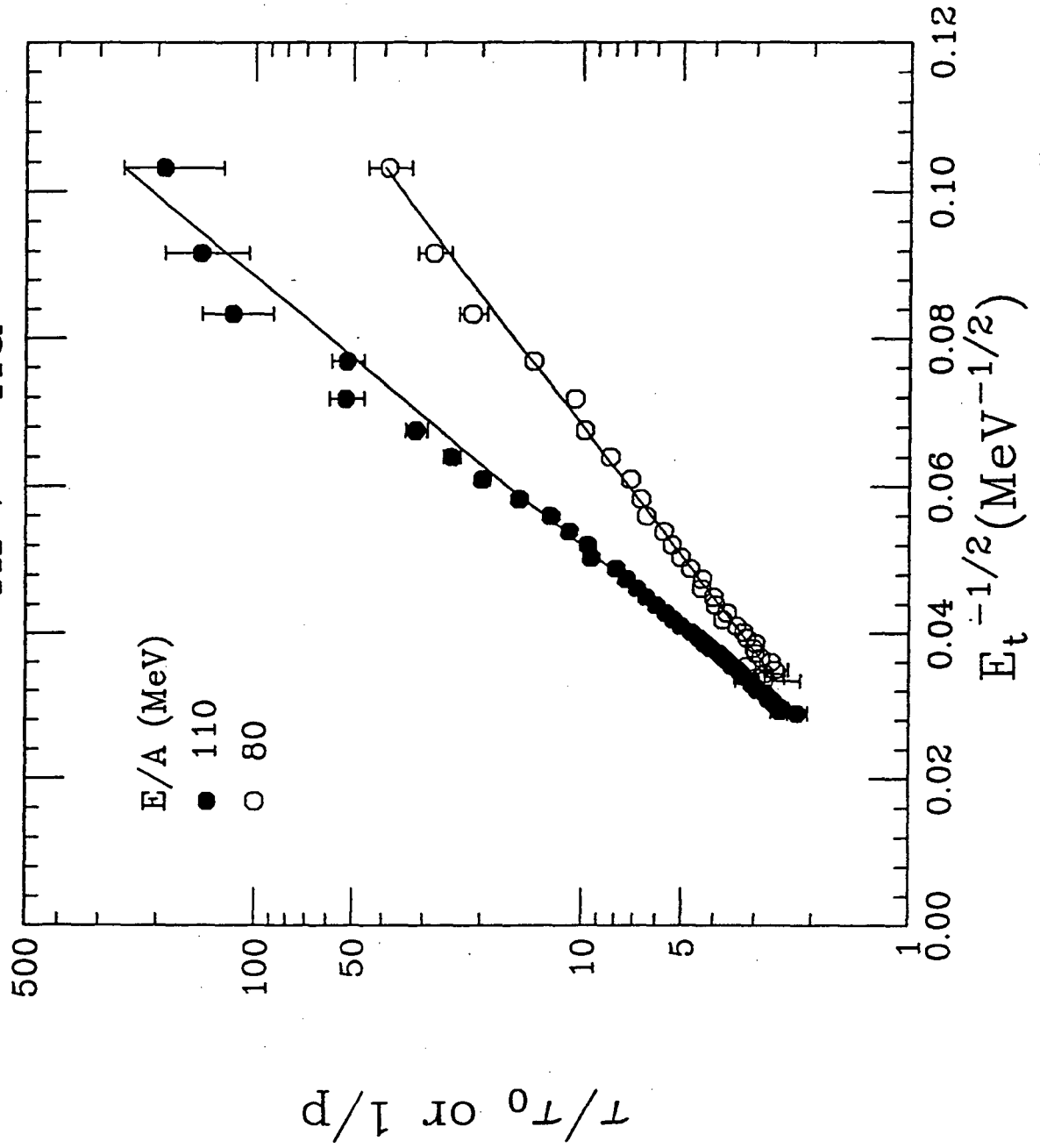[2] L. G. Moretto and G. J. Wozniak, Prog. Part. & Nucl. Phys. 21, 401 (1988) and references therein.

[3] D. N. Delis et al., Nucl. Phys. **A534**, 403 (1991).

[4] C. Gregoire and B. Tamain, Ann. Phys. Fr. **11**, 323 (1986) and references therein.

[5] W. G. Lynch, Ann. Rev. Nucl. Part. Sci **37**, 493 (1987) and references therein.

[6] D. Guerreau, *Formation and Decay of Hot Nuclei: The Experimental Situation*   (Plenum Publishing Corp., 1989).

[7] H. H. Gutbrod, A. M. Poskanzer, and H. G. Ritter, Rep. Prog. Phys. **52**, 1267 (1989) and references therein.

[8] D. H. E. Gross, Rep. Prog. Phys. **53**, 605 (1990) and references therein.

[9] L. G. Moretto and G. J. Wozniak, Ann. Rev. Part. & Nucl. Sci **43**, 379 (1993) and references therein.

[10] J. Aichelin, Phys. Rep. **202**, 233 (1991) and references therein.

[11] B. Borderie, Ann. Phys. Fr. **17**, 349 (1992).

[12] O. Schapiro and D. H. E. Gross, Hahn-Meitner-Institut Berlin GmbH, (1994).

[13] T. Ethvignot et al., Phys. Rev **C46**, 637 (1992).

[14] T. Ethvignot et al., Phys. Rev. **C48**, 618 (1993).

[15] D. Fox et al., Phys. Rev. **C47**, R421 (1993).

[16] E. Bauge et al., Phys. Rev. Lett. **70**, 3705 (1993).

[17] D. R. Bowman et al., Phys. Rev. Lett. **70**, 3534 (1993).

[18] T. C. Sangster et al., Phys. Rev. **C47**, R2457 (1993).

[19] M. Louvel et al., Phys. Lett. B **320**, 221 (1994).

[20] M. Abouffirassi et al., LPC Caen, preprint LPCC 94-02 (1994).

[21] A. Lleres et al., ISN Grenoble, preprint ISN 94-33 (1994).

[22] L. G. Moretto, Nucl. Phys. **A247**, 211 (1975).

[23] R. J. Charity et al., Nucl. Phys. **A483**, 371 (1988).

[24] J. Hüfner, Phys. Rep. **125**, 129 (1985) and references therein.

[25] J. P. Bondorf et al., Nucl. Phys. **A443**, 321 (1985).

[26] L. G. Moretto, D. N. Delis, and G. J. Wozniak, Phys. Rev. Lett. **71**, 3935 (1993).

[27] J. Pouliot et al., Phys. Rev. C **48**, 2514 (1993).

[28] L. Phair, Ph.D. thesis, Michigan State University, (1993).

[29] L. Phair et al., Phys. Lett B **291**, 7 (1992).

[30] R. Bougault et al., Laboratoire de Physique Corpusculaire, preprint LPCC 94-04 (1994).

[31] R. T. deSouza et al., Nucl. Instr. and Meth. **A295**, 109 (1990).

[32] L. Phair, R.T. de Souza, D.R. Bowman, C.K. Gelbke, W.G. Gong, Y.D. Kim, M.A. Lisa, W.G. Lynch, G.F. Pealsee, M.B. Tsang and F. Zhu, to be published (private communication).

[33] D. N. Delis et al., to be published (private communication).

[34] K. Tso et al., to be published (private communication).
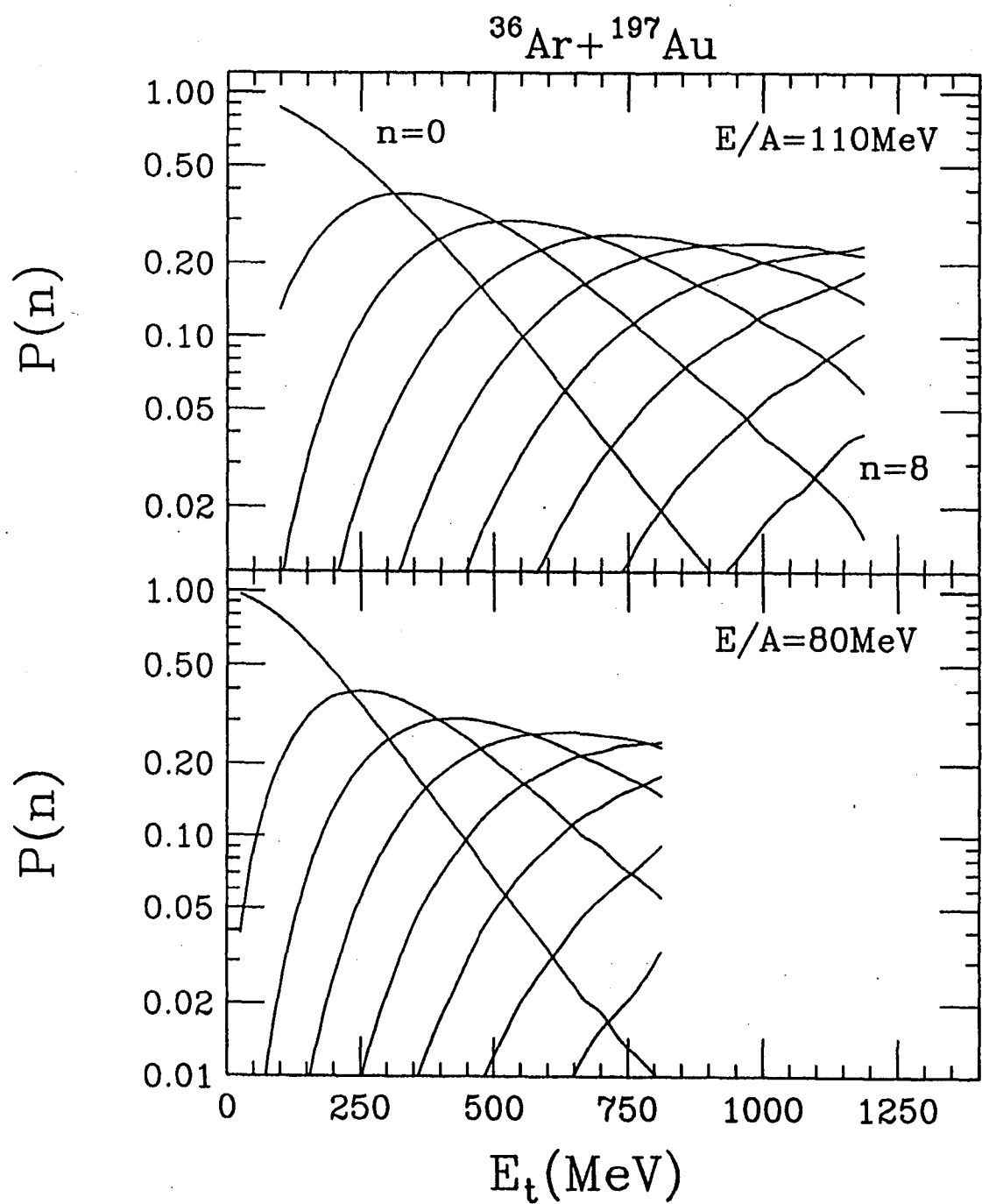
[35] W. A. Friedman, Phys. Rev. **C42**, 667 (1990).

$^{36}Ar + ^{197}Au$

E/A (MeV)
● 110
○ 80

$E_t \, (MeV)$

m

XBL 944-220

9

$^{36}Ar + {}^{197}Au$

E/A (MeV)
● 110
○ 80

τ/τ_0 or $1/p$

$E_t^{-1/2}(MeV^{-1/2})$

XBL 944-221

10

$^{36}Ar + ^{197}Au$

n=0

E/A=110MeV

n=8

E/A=80MeV

$E_t(MeV)$

XBL 944-219